

# Application of machine learning methods for the classification of vibroacoustic signals measured at the moment of transformer energization with varying degrees of core and winding defect complexity

**Abstract.** The research subject is a power transformer, with the goal of identifying and classifying various technical conditions, including the normal state and defects in the core and windings. The aim is to explore various machine learning algorithms, the impact of three different Hamming window sizes for spectral estimation (used as the feature set), and the influence of the number of classes in classification. The study confirms the hypothesis that it is feasible to effectively identify specific types of transformer defects based on vibroacoustic signals.

**Streszczenie.** Przedmiotem badań jest transformator mocy, a celem jest identyfikacja i klasyfikacja różnych stanów technicznych, w tym stanu normalnego oraz wad rdzenia i uzwojeń. Celem prac jest zbadanie różnych algorytmów uczenia maszynowego, wpływu trzech różnych rozmiarów okna Hamminga na estymację spektralną (używaną jako zestaw cech) oraz wpływu liczby klas w klasyfikacji. Badanie potwierdza hipotezę, że możliwe jest skuteczne identyfikowanie konkretnych rodzajów wad transformatora na podstawie sygnałów wibroakustycznych. (Zastosowanie metod uczenia maszynowego do klasyfikacji sygnałów wibroakustycznych mierzonych w momencie zasilania transformatora o różnym stopniu złożoności uszkodzeń jego rdzenia i uzwojeń).

**Słowa kluczowe:** metoda wibroakustyczna, pomiar drgań, transformator, rdzeń, uzwojenie, klasyfikacja, uczenie maszynowe.

**Keywords:** vibroacoustic method, vibration measurement, transformer, core, winding, classification, machine learning.

## Introduction

In recent years, the modified vibroacoustic method for assessing the technical condition of transformer cores and windings has been developing rapidly [1-4]. This method is gaining popularity due to its precision and reliability in damage diagnostics. One of the key aspects of this development is evaluating the potential of using selected machine learning tools for classifying vibroacoustic signals recorded during the transformer's startup. These tools enable the recognition of core and/or winding defects of varying complexity. The introduction of advanced algorithms allows for precise signal analysis, significantly enhancing diagnostic effectiveness [5-9]. The next step in refining this method is to try to make the process of identifying the complexity of mechanical defects in the transformer core and/or windings independent of the subjective assessment of a diagnostician (expert). Automating this process with machine learning tools minimizes the influence of human factors and eliminates the risk of errors stemming from subjective evaluations. The automation of the fault classification process for the active parts of the transformer, based on the analysis of vibroacoustic signals measured at startup, represents a milestone in transformer diagnostics. This allows for quick and efficient fault detection, increasing the reliability and safety of these devices. The modified vibroacoustic method supported by machine learning tools opens new possibilities in the diagnostics of power transformers [10-13]. Automation and independence from expert subjective assessments are key elements that contribute to increasing the efficiency and precision of evaluating the technical condition of these critical components in the energy infrastructure.

The challenge involves the necessity of selecting appropriate features and classification methods, as we have only a limited amount of training data. The objective is to investigate various machine learning algorithms, to examine the impact of three different Hamming window sizes for spectral estimation, which serves as the feature set for the classifier, and to study the influence of the number of classes in classification. These classes are related to the type of defect, its source, and the transformer's condition,

representing different levels of diagnostic detail for the transformer.

## The object under study and the measurement system

The subject of the research is a power transformer manufactured in 1970, which had the following parameters: made by Elta Łódź, type TONb-100/20; rated power 100 kVA; voltage ratio 15/0.4 [kV/kV]; HV current 3.85 [A]; LV current 144 [A]; connection group - Yz5. The research task aims to identify and classify various technical conditions of the transformer, including the normal state and defects in the core and windings, by utilizing advanced algorithms and machine learning. In the study, two sources of defects were considered: winding defects and core defects. Regarding winding defects, studies indicate [14-17] that mechanical issues in transformer windings, such as deformation, displacement, and loosening of clamping force, can significantly impact the vibration profile. Analysis of the spatial distribution of winding vibrations under various loading conditions has shown that these defects lead to alterations in the vibration characteristics of the transformer tank. Similar to windings, core defects like loosening or displacement affect the vibration distribution. Advanced signal analysis techniques, such as Fourier transform and wavelet analysis, enable the identification and classification of these defects, which is crucial for reliable transformer diagnostics [18-21]. The visualization of the examined device with the marked individual defects is shown in Fig. 1.

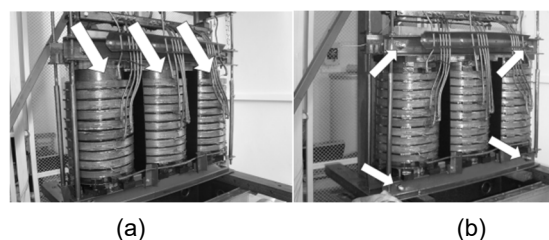


Fig.1. Photo of the examined object with modelled defects: a) winding defects, b) core defects.

The study investigated 18 different states of the transformer's technical condition, including 8 types of defects in the no-load condition, 8 types of defects under load, and normal operation (without defects) in the no-load condition and under load. In each state (idle and under load), simulating nine different types of defects, the transformer was activated ten times, with vibroacoustic signals recorded by four sensors placed in various locations and configurations. A total of 720 measurements were collected and used for analysis. Measurements from the ten activations were combined into a single group, regardless of the sensor location, resulting in 80 measurements for each defect.

Table 1 lists the types of modelled conditions. As shown in Table 1, the designations are categorized based on the number of recognized conditions: D18, D9, D4, and D2. Each designation represents a different set of conditions, with D18 indicating 16 various defects identified in the transformer and 2 no-defect conditions, D9 indicating 8 defects and 1 no-defect condition, D4 indicating 2 defects

and 1 no-defect condition, and D2 indicating 2 conditions (either a defect exists in the transformer or it does not). This classification helps in analysing the impact of varying defect quantities on the classification performance. In the case of group D9, signals were combined regardless of the transformer's state (loaded or unloaded), aiming to generalize the diagnosis independently of the operating condition. For group D4, signals recorded for different types of core damage and winding damage were combined separately. For group D2, which represented the highest level of generalization, all types of defects were combined with signals recorded during defect-free operation.

The measurement system comprises a setup designed to capture and analyse vibroacoustic signals generated during the operation of transformers. Fig. 2 shows a general view of the four-channel transformer vibration measurement system that was used during the research experiment.



Fig.2. Photo of the test setup.

Table 1. Designations of modelled defects depending on the number of recognized technical conditions: D18, D9, D4, and D2.

Type of Modeled Defect	Number of conditions classified				
	D18		D9	D4	D2
	Load	No-load			
Device without defect	LND	NND	ND	ND	ND
Loosened right upper core yoke screw	LCD1	NCD1	CD1	C	D
Loosened right upper and left upper core yoke screws	LCD2	NCD2	CD2		
Loosened right upper, left upper, and lower left core yoke screws	LCD3	NCD3	CD3		
Loosened right upper, left upper, lower left, and lower right core yoke screws (all core yoke screws loosened)	LCD4	NCD4	CD4		
Loosened winding coil of phase L1	LWD1	NWD1	WD1	W	
Loosened winding coils of phase L1 and phase L3	LWD2	NWD2	WD2		
Loosened winding coils of phase L1, phase L2, and phase L3	LWD3	NWD3	WD3		
All four core yoke screws loosened, all winding coils of phases L1, L2, and L3 loosened	LCW	NCW	CW	CW	

This setup includes sensors for detecting vibrations - accelerometers Briel&Kjael type 4514, data acquisition hardware to record the signals - system Pulse DynXI 3050, and software tools for processing and analysing the data - Time Data Recorder by Briel&Kjael. The integration of this system into transformer diagnostics involves several key components. High-sensitivity accelerometers used to capture vibrations from the transformer. These sensors are strategically placed to detect signals indicative of potential defects. The captured signals are recorded using high-speed data acquisition hardware - Pulse DynXI measuring cassette, type 3050, manufactured by Bruel&Kjael, ensuring that the signals are sampled at an appropriate rate to capture all relevant details. The load on the tested 100 kVA transformer was applied using a second 250 kVA transformer (achieved by connecting the 6 kV windings of both transformers in series, with the supply to the tested transformer being 0.4 kV). The induction of an impulse current in the windings of the tested transformer aimed to generate vibrations in its windings, proportional to the square of the surge current. Due to the impulsive nature of the load current, its high rate of change, and the generation of an overvoltage wave, the load power was not measured. However, it is estimated to be between several dozen to several hundred kVAR.

Example time waveforms of vibroacoustic signals are presented in Fig. 3 for: a) signal registered in the no-load condition of the transformer, with loosened right upper core yoke screw (NCD1) and b) signal registered in the no-load condition of the transformer, without any defect (NND).

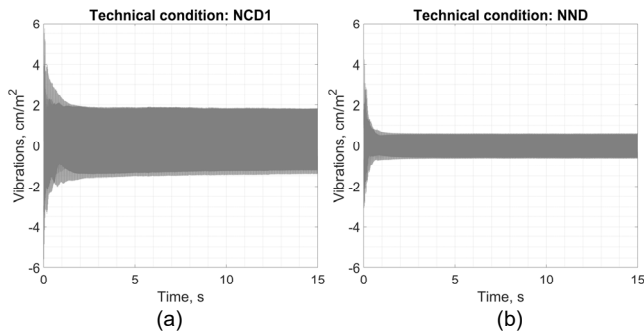


Fig.3. Example time series for NCD1(a) and NND (b) device operation.

### Feature extraction and classification procedure

In the procedure of feature extraction from recorded vibroacoustic signals, spectral components were determined. To estimate the power spectral density, the method proposed by Peter Welch, which is an improvement of the periodogram method, was applied. This method involves dividing the signal into several short, overlapping segments, which helps reduce the variance of the spectral estimate. Each segment is then multiplied by a window function to reduce the spectral leakage effect that can occur due to the finite length of the segments. The power spectrum is calculated for each segment, and then the power spectral density estimate is obtained by averaging the spectra from all segments. In the study, the Hamming window function was used, which has the ability to suppress side lobes in the signal spectrum, helping to reduce spectral leakage while maintaining the main lobe width at an acceptable level. Three different window sizes were considered: H1-Hamming (1024), H2-Hamming(512), and H3-Hamming(256). The visualization of spectra calculated using three windowing methods is shown in Fig. 4 for NCD1 and NND, respectively.

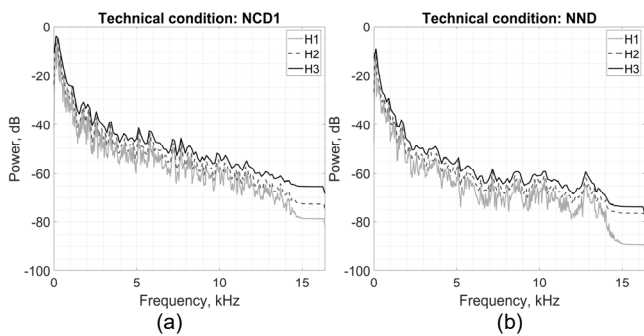


Fig.4. Example power spectra estimates: a) NCD1, b) NND.

The classification procedure is illustrated in Fig. 5 as flowchart. It illustrates the steps involved in training and evaluating machine learning models for classifying transformer defects based on vibroacoustic signals. The process begins with the collection of measurement data, followed by the generation of unique features. The core of the process is the Monte Carlo validation, which includes 100 iterations. Within each iteration, training and testing sequences are randomly selected in a 70/30 ratio. The machine learning algorithms are then trained and tested, and the classification quality metrics are calculated. Finally, the best model is selected based on the calculated metrics.

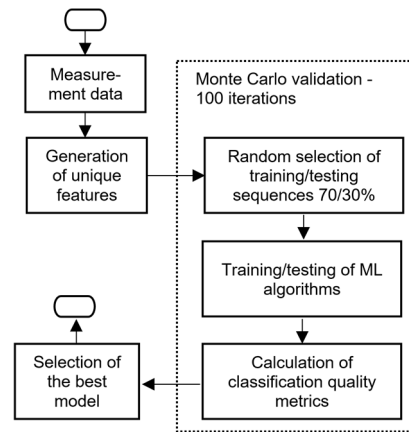


Fig.5. Flowchart of the machine learning model training and evaluation process.

The following machine learning algorithms were applied during the research: a decision tree utilizing the Gini Impurity splitting criterion with a maximum of 100 splits (Tree); an ensemble of 30 decision trees sampled randomly with replacement (EnBagT), and sampled using the Random Under-Sampling Boosting method (EnBooT), aggregated via majority voting; an ensemble of 30 linear discriminant classifiers (EnDis); an ensemble of 30 k-nearest neighbors classifiers with  $k=1$  (EnKnn); a k-nearest neighbors algorithm with  $k=1$ , utilizing Euclidean distance and equal weights (Knn); neural networks with 10 (10xNN), 100 (100xNN), and 200 (200xNN) neurons in a single hidden layer, employing the Rectified Linear Unit activation function and a regularization parameter of  $\lambda=0.001$ ; and support vector machines with a linear kernel (SvmL), a polynomial kernel of degree 2 (SvmQ), and a polynomial kernel of degree 3 (SvmC).

The following evaluation metrics were applied for classifier evaluation: accuracy (indicates the ratio of correctly predicted observations to the total number of observations, can be misleading in cases of imbalanced datasets), sensitivity (assesses the model's ability to correctly identify positive cases, low value indicates false negative cases), specificity (assesses the model's ability to correctly identify negative cases, low value indicates false positive cases), precision (assesses the model's effectiveness in identifying positive results only among the cases that the model classified as positive), F1 score (represents the harmonic mean of precision and sensitivity, effective in imbalanced datasets), Matthews correlation coefficient (considers all elements of the confusion matrix).

Figure 6 and 7 present example results depicting boxplots of the six considered classification metrics, where each metric is evaluated for four different technical conditions of the transformer (D4) in Fig. 6 and for nine different technical conditions of the transformer (D9) in Fig. 7.

The in Fig. 6 presented boxplots provide the following insights. The MCC boxplots show that all technical conditions (C, ND, CW, W) have relatively high values, with some variation. The C condition tends to have slightly lower MCC values compared to the others. The F1 Score boxplots demonstrate that all conditions achieve high values, with the ND condition slightly outperforming the others, indicating a good balance between precision and recall across conditions. For Sensitivity, the ND and C conditions show higher values, indicating that the classifier is particularly good at identifying these conditions. The W condition has the widest range of sensitivity values,

showing more variability. The boxplots indicate high specificity across all conditions, with very little variability, suggesting that the classifier is effective at identifying true negatives in all cases. The ND condition has the highest precision, indicating that when the classifier predicts no defect, it is very likely to be correct. Other conditions show slightly lower, but still high, precision values. All conditions exhibit high accuracy, with the ND condition again showing slightly better performance. The C condition shows slightly more variability in accuracy. Overall, the boxplots suggest that the classification system performs well across all technical conditions, with particularly strong performance in the ND condition. While there is some variability in sensitivity and precision, the metrics indicate a robust classification system. The results highlight the system's ability to accurately and reliably identify both defective and non-defective states of the transformer.

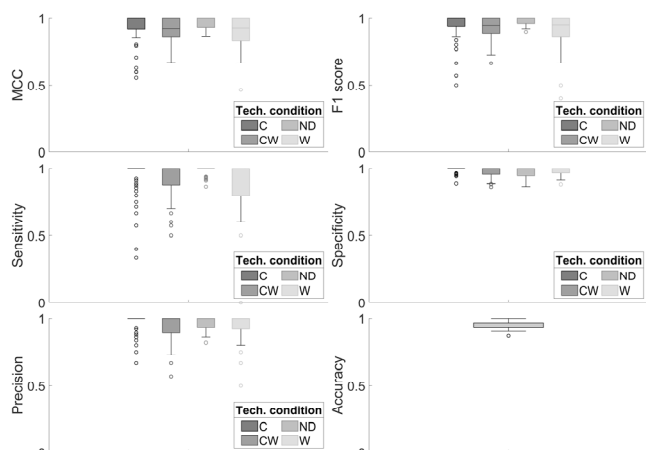


Fig.6. Example boxplots of the classification metrics for four technical conditions (D4), calculated using a neural network with 10 neurons in the hidden layer.

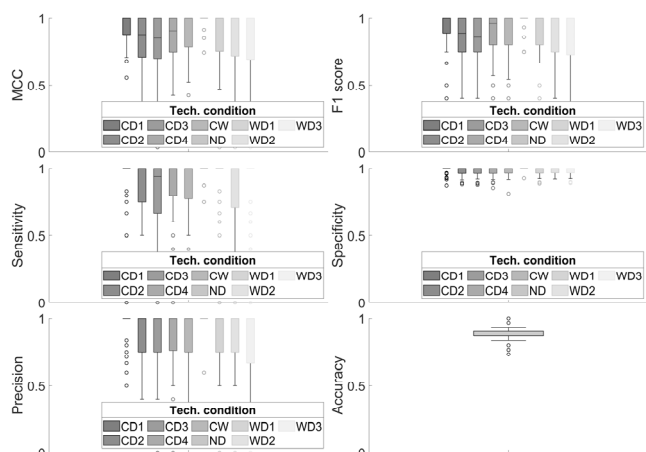


Fig.7. Example boxplots of the classification metrics for nine technical conditions (D9), calculated using a neural network with 10 neurons in the hidden layer.

The analysis of the boxplots presented in Fig. 7 leads to the conclusion that overall, the classifier demonstrates strong performance across all technical conditions, with consistently high values in MCC, F1 Score, Sensitivity, Specificity, Precision, and Accuracy. However, it is important to note the variability within some metrics. For instance, the Sensitivity and Precision metrics show more significant fluctuations across different technical conditions.

To summarize all the conducted research and analyses, Figure 8 presents heatmap depicting the arithmetic mean values of all calculated classification quality metrics, determined over 100 iterations of testing classification algorithms for various methods, hamming window sizes, and classified condition states: D18, D9, D4 and D2. The columns labelled H1 to H3 represent different sizes of the Hamming window used for feature extraction, based on which transformer technical conditions were classified.

Algorithm	D18			D9			D4			D2		
	H1	H2	H3	H1	H2	H3	H1	H2	H3	H1	H2	H3
10xNN	0.87	0.81	0.74	0.95	0.91	0.9	0.95	0.94	0.93	0.92	0.91	0.91
100xNN	0.89	0.86	0.78	0.95	0.92	0.92	0.95	0.95	0.94	0.92	0.91	0.92
200xNN	0.89	0.86	0.79	0.95	0.93	0.92	0.95	0.95	0.94	0.92	0.9	0.92
EnDis	0.46	0.47	0.47	0.63	0.63	0.63	0.53	0.54	0.53			
EnKnn	0.44	0.45	0.45	0.53	0.54	0.57	0.55	0.56	0.58	0.68	0.66	0.66
EnBagT	0.76	0.73	0.74	0.89	0.86	0.86	0.91	0.89	0.9	0.84	0.84	0.85
EnBooT	0.67	0.67	0.69	0.85	0.82	0.83	0.93	0.9	0.92	0.91	0.89	0.9
SvmL	0.82	0.77	0.75	0.91	0.87	0.85	0.91	0.87	0.85	0.85	0.8	0.8
SvmQ	0.88	0.83	0.84	0.95	0.92	0.92	0.95	0.93	0.93	0.9	0.89	0.88
SvmC	0.85	0.83	0.82	0.94	0.92	0.91	0.95	0.93	0.93	0.92	0.91	0.9
Tree	0.62	0.58	0.66	0.79	0.76	0.75	0.78	0.81	0.79	0.8	0.79	0.78
Knn	0.79	0.77	0.74	0.9	0.91	0.88	0.91	0.93	0.91	0.91	0.93	0.92

Fig.8. The arithmetic mean values of all calculated classification quality metrics, determined over 100 iterations for various algorithms, hamming window sizes, and classified condition states.

Based on the presented aggregate results, the following conclusions can be drawn. As the number of classes decreases from D18 to D2, the classification accuracy generally increases across all algorithms, indicating that simpler classification tasks (fewer classes) yield higher accuracy. In general, H1 seems to provide slightly higher accuracies compared to H2 and H3 for most algorithms, although the difference is not very pronounced. Some algorithms consistently perform better than others. For example, SvmC and SvmQ show high accuracies across all conditions, while EnDis and EnKnn show lower accuracies. Specific algorithms like 10xNN, 100xNN, and 200xNN demonstrate high and consistent performance across various window sizes and classification levels. The key observations are as follows: the SvmC and SvmQ algorithms exhibit robust performance across all window sizes and classification levels, suggesting they might be more reliable for this type of classification task; the EnDis algorithm shows notably lower performance, indicating it may not be well-suited for this application; The impact of Hamming window size on classification accuracy is present but not overly significant, with H1 slightly outperforming H2 and H3 in many cases.

### Conclusions and further research steps

The study confirms the hypothesis that it is feasible to effectively identify specific types of transformer defects based on vibroacoustic signals. Overall, classification accuracy tends to improve as the number of classified conditions decreases from D18 to D2. Increasing the diagnostic accuracy by recognizing more classes with a limited number of measurements results in a reduction in the average effectiveness. Reducing the window size leads to a decrease in the number of details that serve as unique features of defects, thereby negatively affecting the overall classification accuracy. Among the different Hamming window sizes, H1 generally yields slightly better results. The highest average accuracy was observed with feature window sizes of 1024 (H1) and 512 (H2) when recognizing D4 and D9 conditions of the transformer, utilizing neural

networks and support vector machines. Algorithms like SvmC and SvmQ consistently achieve high accuracy, making them favourable choices for classifying transformer defects based on vibroacoustic signal analysis. Additionally, algorithms such as 10xNN, 100xNN, and 200xNN demonstrate strong performance across various Hamming window sizes and classification levels.

Future research should focus on conducting additional measurements in both existing and novel systems that simulate defects. Furthermore, calculating and examining the impact of new features, such as wavelet transforms and spectrograms, on classification effectiveness is essential. It is also crucial to validate the developed models under real-world conditions to ensure their robustness and reliability. Finally, implementing the developed model into an expert system within the industry will facilitate practical applications and enhance defect detection processes.

**Authors:** prof. dr hab. inż. Sebastian Borucki, E-mail: s.borucki@po.edu.pl; prof. dr hab. inż. Jerzy Skubis, E-mail: j.skubis@po.edu.pl; dr hab. inż. Daria Wotzka, E-mail: d.wotzka@po.edu.pl; prof. dr hab. inż. Dariusz Zmarzły, E-mail: d.zmarzly@po.edu.pl; Politechnika Opolska, Katedra Elektroenergetyki i Energii Odnawialnej, ul. Prószkowska 76, 45-758 Opole.

#### REFERENCES

- [1] Secic A., Krpan M., Kuzle I., Vibro-Acoustic Methods in the Condition Assessment of Power Transformers: A Survey, *IEEE Access*, 7 (2019), 83915-83931
- [2] Krupinski R., Kornatowski E., Analysis of the GGD Vibroacoustic Detector of Power Transformer Core Damage, *IEEE Access*, 12 (2024), 45752-45761
- [3] Kornatowski E., Detection of the Transient Vibrations Amplitude of Power Transformer's Active Part, *Advanced Solutions in Diagnostics and Fault Tolerant Control*, 635 (2018), 169-179
- [4] Borucki S., Cichoń A., The influence of the power transformer load on vibroacoustic signal analysis results, *Przegląd Elektrotechniczny*, 86 (2010), no. 7, 45-47
- [5] Bigdeli M., Siano P., Alhelou H., Intelligent Classifiers in Distinguishing Transformer Faults Using Frequency Response Analysis, *IEEE Access*, 9 (2021), 13981-13991
- [6] Forouhari S., Abu-Siada A., Application of adaptive neuro fuzzy inference system to support power transformer life estimation and asset management decision, *IEEE Trans. on Dielect. and El. Ins.*, 25 (2018), no. 3, 845-852
- [7] Ghoneim S., Mahmoud K., Lehtonen M., Darwish, M., Enhancing Diagnostic Accuracy of Transformer Faults Using Teaching-Learning-Based Optimization, *IEEE Access*, 9 (2021), 30817-30832
- [8] Wotzka, D., Sikorski, W., Szymczak, C., Investigating the Capability of PD-Type Recognition Based on UHF Signals Recorded with Different Antennas Using Supervised Machine Learning, *Energies* 15 (2022), no. 3167
- [9] Wotzka, D., Cichoń, A., Study on the Influence of Measuring AE Sensor Type on the Effectiveness of OLTC Defect Classification, *Sensors* 20 (2020), no. 3095
- [10] Ji S., Zhu L., Li, Y., Study on transformer tank vibration characteristics in the field and its application, *Przegląd Elektrotechniczny*, 87 (2011), no 2, 205-211
- [11] Hu, J., Liu, D., Liao Q., Yan Y., Liang S., Electromagnetic vibration noise analysis of transformer windings and core, *IET Electric Power Application*, 10 (2016), no. 4, 251-257
- [12] Würde A., Kahlen J., Langenberg N., Moser A., Transformer Core-Vibration Analysis: Coupling Paths, in. *2022 IEEE Electrical Insulation Conference (EIC)*, Knoxville, USA, (2022)
- [13] Hu, Y., Zheng, J., Huang, H., Experimental Research on Power Transformer Vibration Distribution under Different Winding Defect Conditions, *Electronics*, 8 (2019), no. 8, 1-19
- [14] García B., Burgos J., Alonso A., Winding deformations detection in power transformers by tank vibrations monitoring, *Electric Power Systems Research*, 74 (2005), no. 1, 129-138
- [15] Borucki S., Cichoń A., Majchrzak H., Zmarzły D., Evaluation of the Technical Condition of the Active Part of the High Power Transformer Based on Measurements and Analysis of Vibroacoustic Signals, *Archives of Acoustics*, 42 (2017), no. 2, 313-320
- [16] Duan X., Zhao T., Liu J., Zhang L., Zou L., Analysis of Winding Vibration Characteristics of Power Transformers Based on the Finite-Element Method, *Energies*, 11 (2018), no. 9, 2-19
- [17] Zhou H., Hong K., Huang H., Zhou J., Transformer winding fault detection by vibration analysis methods, *Applied Acoustics*, 114 (2016), 136-146
- [18] Borucki S., Time-Frequency Analysis of Mechanical Vibrations of the Dry Type Power Transformer Core, *Acta Physica Polonica A*, 120 (2011), no. 4, 571 – 574
- [19] Kornatowski E., Banaszak S., Molenda P., Quality Index for Assessment of the Mechanical Condition of Transformers' Active Part with Frequency Response and Vibroacoustic Measurements, *Energies*, 17 (2024), no. 6, 2-17
- [20] Zhou X., Luo Y., Tian T., Bai H., Wu P., Liu W., Transformer fault diagnosis based on probabilistic neural networks combined with vibration and noise characteristics, *Frontiers in Energy Research*, 11 (2023)
- [21] Zhang F., Ji S., Shi Y., Zhan C., Zhu L., Investigation on vibration source and transmission characteristics in power transformers, *Applied Acoustics*, 151 (2019), 99-112